Journal Name

Dynamic Article Links ►

Cite this: DOI: 10.1039/c0xx00000x

www.rsc.org/xxxxxx

ARTICLE TYPE

Self-assembling amphiphilic Janus dendrimers: mesomorphic properties and aggregation in water

Elisabetta Fedeli,[a,b] Alexandre Lancelot,[a,b] José Luis Serrano,[a] Pilar Calvo,[b] Teresa Sierra*[c]

Received (in XXX, XXX) Xth XXXXXXXXX 20XX, Accepted Xth XXXXXXXXX 20XX

DOI: 10.1039/b000000x

The self-assembly behaviour both in bulk and in water of amphiphilic dendrimeric derivatives based on bis-MPA is the central theme of this article. The designed molecules possess two parts with different polarity; this feature is the key factor that forces their self-assembly in water into supramolecular architectures, due to hydrophobic interactions between the lipophilic fractions of the molecules, and the appearance of mesomorphic order in bulk in response to a variation of temperature (thermotropic liquid crystals). The effects provoked by the hydrophilic/lipophilic balance of the molecule were studied varying the generation of the corresponding dendrons and combining them *via* CuAAC click chemistry in order to obtain symmetrical and unsymmetrical final Janus dendrimers. The ability of the aggregates formed in water to encapsulate hydrophobic drugs has also been explored.

Introduction

Dendrimers are monodisperse or nearly monodisperse macromolecules characterized by a regular and highly branched three-dimensional architecture. They consist of three main parts: the multifunctional central core, the interior branches formed by repeating monomeric units and the external functional groups. All the portions of the dendrimer contribute to determine a huge range of nano-physicochemical properties as well as the overall size, shape, reactivity and flexibility.[1-3]

The combination of conventional synthetic approaches, divergent[4,5] or convergent strategies,[6,7] and new synthetic procedures, eg. chemoselective methods (click chemistry),[8-14] allows the realization of *ad-hoc* tailored dendrimers possessing specific and desired features. For instance, the possibility to synthesize separately dendrons with different characteristics and to couple them in the last synthetic step allows the easy production of dendrimers with two different functionalities in two precise areas. Such dendrimers are known as Janus dendrimers.[15]

When the difference between the dendrons composing the dendrimer relies on their polarity, amphiphilic Janus dendrimers are prepared.[16-20] The different polarity between the two blocks of the dendrimer is the key factor that favors the spontaneous self-assembly in water into complex supramolecular structures. The poor affinity of the lipophilic block for the aqueous media provokes the appearance of hydrophobic interactions between the lipophilic fractions of the molecules that tend to hide from the exterior media. The resulting structures present a hydrophilic outer layer that surrounds and stabilizes the lipophilic interior fraction (micelles, vesicles, multi-layered structures, etc.).[21] Moreover, the different affinity between the two blocks can favor also the formation of long-range order in the absence of solvent as response to a variation of the temperature, i.e. thermotropic liquid crystals.[22-23] The structure of the molecule, the characteristics of the blocks and the ratio between the hydrophilic and the lipophilic parts play a crucial role in the determination of the features of the compounds such as their ability to form mesophases and their ability to self-assemble in water forming different architectures.[23]

Furthermore, dendrimers have shown great potential for the design of efficient vehicles for drug delivery, mainly forming either covalent or guest-host drug-dendrimer conjugates.[24] The possibility of Janus-type amphiphilic dendrimers to self-assemble in supramolecular structures makes them excellent candidates to implement nanoaggregates in aqueous solution, which in turn could trap molecules. Amphiphilic dendrimers have been described to form a variety of supramolecular nanostructures,[16,25] enabling the effective internalization of their encapsulated drugs into cells.[26]

In this work, we present a series of amphiphilic Janus dendrimers derived from 2,2-bis(hydroxymethyl)propionic acid (bis-MPA). Bis-MPA based dendrimers exhibit excellent aqueous solubility and are easy to fabricate via convergent or divergent methods. They have proven to be perfectly suitable to build drug carriers[27-28] thanks to their low cytotoxicity and biodegradability. The Janus dendrimers proposed in this article are formed by two bis-MPA dendritic blocks of different polarity (Chart 1). The hydrophilic block consists on a bis-MPA dendron with free terminal –OH groups,[17-19] while, for the lipophilic block, the bis-MPA dendron is functionalized with aliphatic chains derived from stearic acid. The composition of the final Janus dendrimers relies on the combination of equal or different generations of both types of dendron, which are readily linked together with Cu(I)-

catalyzed 1,3-dipolar cycloaddition between alkyne and azide groups (CuAAC).[29]

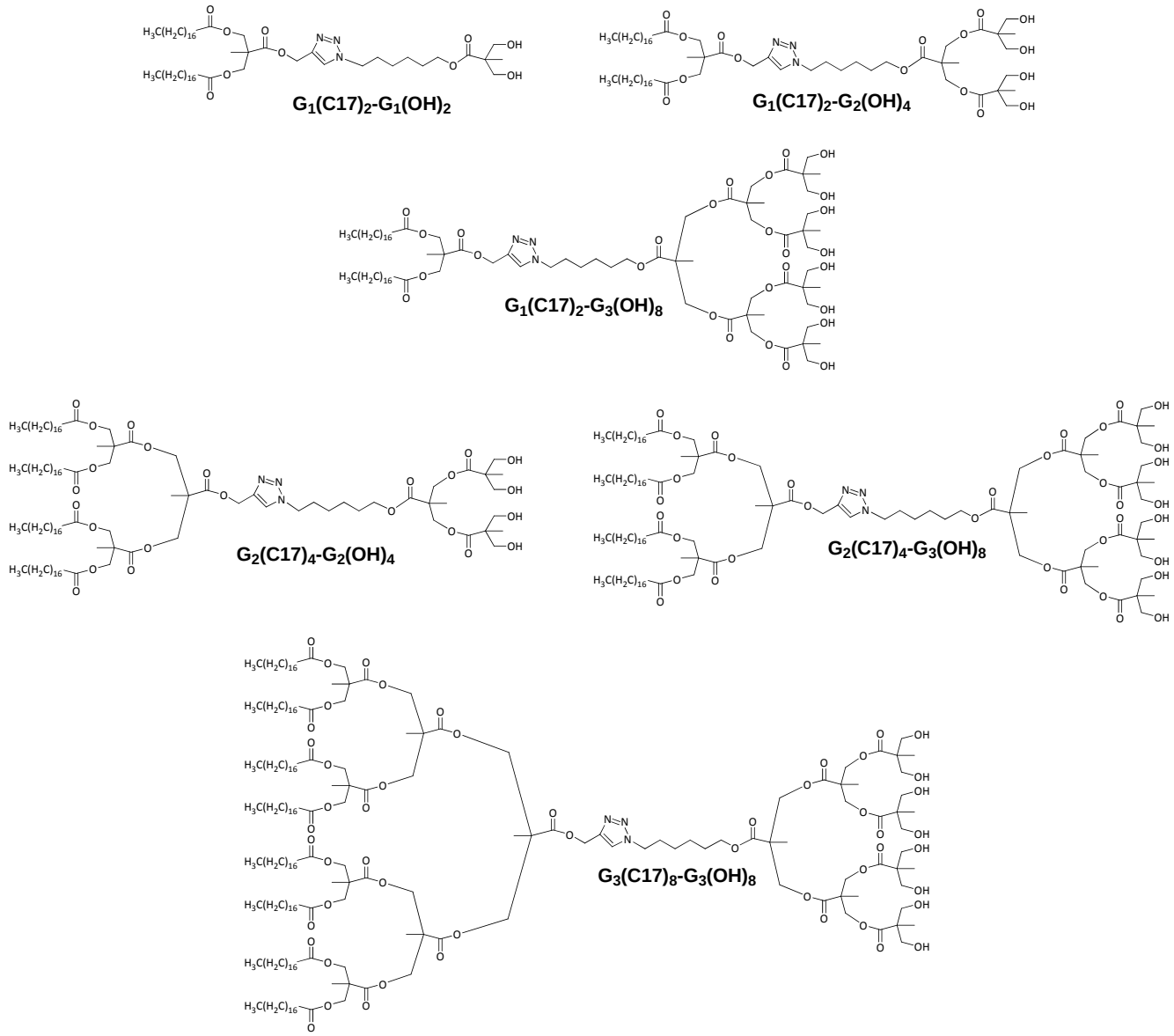

Chart 1 Structure of the amphiphilic Janus dendrimers

Experimental

Materials

6-chlorohexanol, sodium azide, 2,2-Bis(hydroxymethyl)propionic acid (bis-MPA), Stearic acid, Pd/C, $CuSO_4$, sodium ascorbate, N,N'-dicyclohexylcarbodiimide (DCC) were purchased from Aldrich and used without further purification. Anhydrous CH_2Cl_2 was purchased from Scharlab and dried using a solvent purification system. Plitidepsin was supplied by Pharma Mar and used without further purification. Ultrapure Milli-Q water (ρ= 18.2 $M\Omega \cdot cm^{-1}$) was used to favor the formation of aggregates.

Synthesis

In order to perform the CuAAC reaction in the final step of the dendrimer synthesis, both types of dendron were synthesized separately and functionalized on the focal point with the necessary groups: an alkyne group for the lipophilic block and an azide group with a hexamethylenic spacer for the hydrophilic block. The synthesis of the dendrons followed the divergent method, adapting reactions published in the literature,[30] and the generation was grown following the Steglich method,[31] which employs dicyclohexylcarbodiimide (DCC) and 4-(dimethylamino)pyridinium p-toluenesulfonate (DPTS) as activating agents.

Aggregates formation, TEM and encapsulation studies

The formation of aggregates was carried out employing the oil-in-water method. Each amphiphlic compound was dissolved in a volatile, non-water-soluble solvent, then milli-Q water was added and the mixture stirred rapidly until complete evaporation of the organic fraction (see the ESI).[32]

The morphology of the aggregates formed after the self-

assembly of the Janus dendrimers in water was studied with the aid of Transmission Electron Microscopy (TEM) using uranyl acetate 0.1 N as negative stain.

The encapsulation procedure was performed employing the oil-in-water method explained before and adapted for this specific procedure. The amphiphilic compound was dissolved in dichloromethane at 0.5µmol/mL. In order to exploit the complete payload capacity of the aggregates, a concentration of Plitidepsin of 1 µmol/mL, was chosen to perform the encapsulation (see the ESI).

Results and discussion

Synthesis and characterization

The synthesis of the dendrons started with the selective protection of the hydroxyl groups of the bis-MPA as acetals. In the following step, the focal point of this compound was functionalized with an alkyne group in the case of the lipophilic dendrons and with an azide group through an hexamethylenic spacer in the case of the hydrophilic dendrons.

The first three generations of both dendrons were obtained employing the divergent approach, alternating steps of growth of the generation via the Steglich esterification with *N,N'*-dicyclohexylcarbodiimide (DCC) and 4-(dimethylamino) pyridinium 4-toluenesulfonate (DPTS) and steps of deprotection of the hydroxyl groups with Dowex (Scheme 1). In the case of the lipophilic dendrons, the functionalization of the periphery of the dendrons with stearic acid chains was performed via Steglich esterification in the final step.

The characterization of all the compounds was performed via ^{1}H-NMR, ^{13}C-NMR, FTIR, GPC and MS (see the ESI). The characterization by FTIR spectroscopy of the hydrophilic dendrons revealed the presence of the azide group through an intense sharp peak at 2092 cm^{-1} that corresponds to the stretching vibration of the -N=N^{+}=N- bonds. A proof of the presence of free hydroxyl groups on the periphery of the dendron was the wide band recorded at approximately 3200 cm^{-1} associated to the stretching vibration of the O–H bond (Fig S3-1 in the ESI).

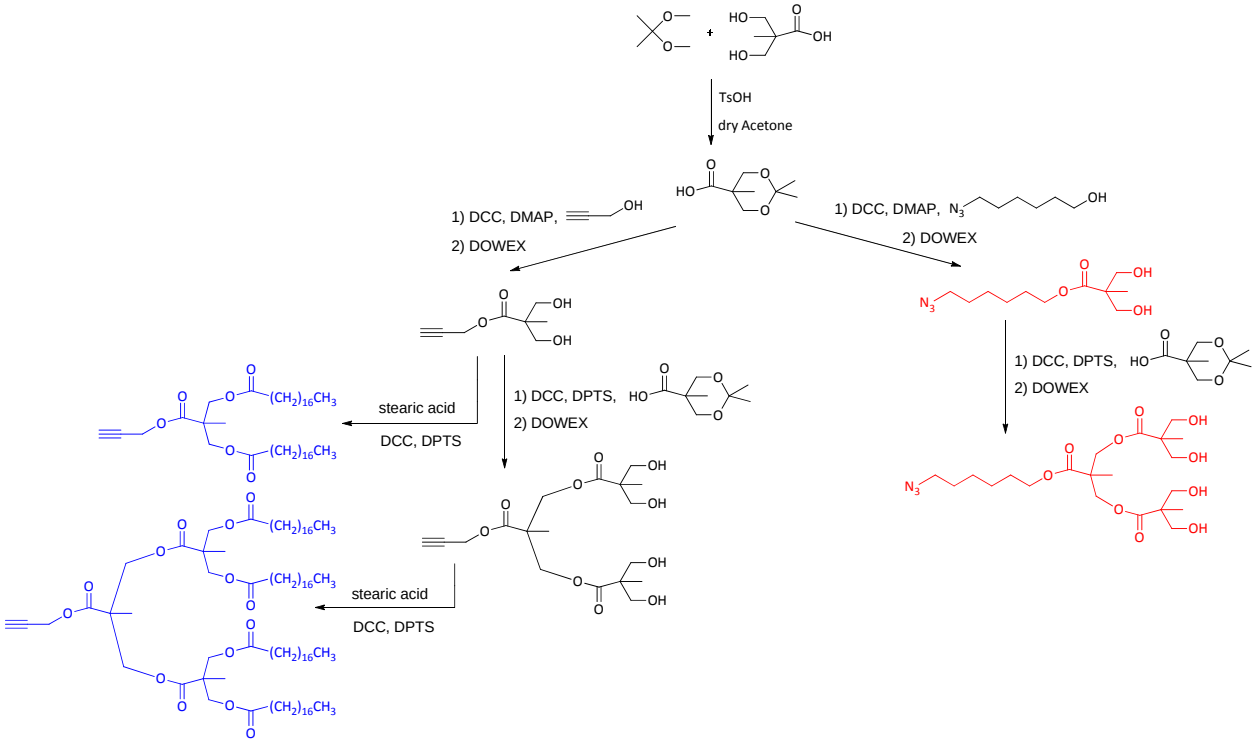

Scheme 1 Divergent approach employed to synthesize the dendrons til the second generation

The FTIR characterization of the lipophilic dendrons confirmed the presence of the alkyne group through the observation of a small sharp peak at ca. 3300 cm^{-1}, related to the stretching vibration of the ≡C-H bond. The presence of the aliphatic chains produces a noticeable increase in the intensity of the band relative to the symmetric and asymmetric stretching vibration of the -C-H bonds (2950-2850 cm^{-1}). The presence of unique species with precise molecular weight was confirmed by gel permeation chromatography (GPC), which showed a single sharp symmetric peak, and by mass spectrometry (MS), which detected only the [M+Na]$^{+}$ peak. No peaks, relative to incomplete products or starting reagents, were present (ESI).

The final Janus dendrimers (Chart 1) were obtained by coupling of two dendrons of opposite polarity via CuAAC click chemistry. The catalytic system chosen to run the CuAAC reaction was $CuSO_4 \cdot 5H_2O$ as source of Cu(II) and sodium ascorbate as reducing agent for the production of the Cu(I) species; the solvent was a mixture of dichloromethane, dimethylformamide and water in a ratio 8:1:1, respectively. The reaction mixture was stirred for 48 hours and the temperature was varied depending on the cases (the specific conditions used for each product are reported in the ESI, S3). The purification of the products was performed by washing the reaction mixture with a water solution of KCN that, being able to form a stable complex with Cu(I), allowed the elimination of

copper traces from the solution. The elimination of remaining starting material was achieved, in general, by recrystallization of the product from hexanes and/or by precipitation of the product dissolved in dichloromethane with cold methanol.

The successful formation of the triazole ring and the disappearance of the starting materials were deduced from FTIR spectra (Fig. S3-1 in the ESI) by the absence of the two main characteristic signals of the starting dendrons: the peak relative to the stretching vibration of the -N=N$^+$=N- bonds of the azide group (2092 cm^{-1}), and the peak of the H-C stretching vibration of the alkyne group of the lipophilic dendron (3200 cm^{-1}).

^{1}H NMR helped to confirm the formation of the Janus dendrimer. Compound **$G_2(C17)_4$-$G_3(OH)_8$** is used to explain the ^{1}H NMR study (Fig. 1). The formation of the Janus dendrimer is confirmed by three main signals due to the hydrogens **a**, **b** and **c**. The peak recorded at δ_H=7.59 ppm (s, 1H; **a**) corresponds to the formation of the heterocycle as a linker between the two dendrons. The formation of the triazole ring also provokes the downfield shift of the peaks due to **b** hydrogens (from δ_H=4.72 ppm to δ_H=5.23 ppm) and **c** hydrogens (from δ_H=1.62 ppm to δ_H=1.95 ppm.) with respect to the starting dendrons. Also the signals related to **d** and **e** protons suffer small downfield shifts to δ_H=1.66 ppm and δ_H=1.58 ppm, respectively.

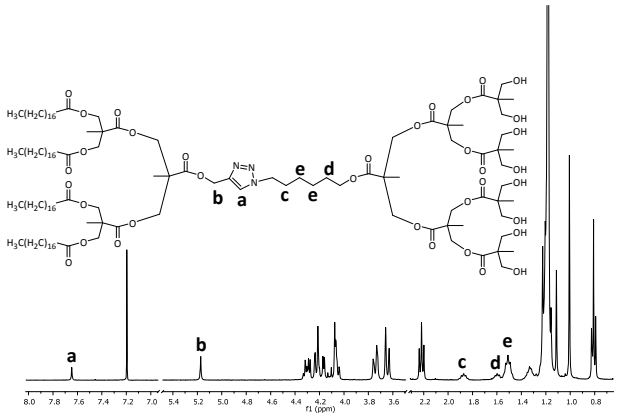

Fig. 1 ^{1}H-NMR spectrum of **$G_2(C17)_4$-$G_3(OH)_8$**, representation of the molecular structure and assignation of the signals to their corresponding hydrogens.

The GPC of the final amphiphilic Janus dendrimers present a unique monomodal and symmetric peak confirming the presence of a single species with a precise molecular weight. The peaks corresponding to the starting materials were not detected and the one relative to the Janus dendrimer appeared, as expected, at lower retention time (Fig. S3-2 in the ESI). In the MS spectra, the presence of a single peak corresponding to [M+Na]$^+$ (Figure S3-3), confirmed the correct formation of the final product and the absence of starting materials. Compound **$G_1(C17)_2$-$G_3(OH)_8$** represents an exception since its MS spectrum presents a distribution of peaks due the high power required for the ionization of the compound that provokes fractures on the molecule resulting in a distribution of peaks (Fig. S3-4 in the ESI).

Thermal and Mesomorphic Properties

The microsegregation between units of different nature present in the structure of the dendrimeric molecule is the driving force that can promote mesomorphic behavior. The study of the thermal behavior of the Janus dendrimers started with the evaluation of the thermal stability of both starting reagents and final compounds by thermogravimetric analysis (TGA). All the compounds presented good thermal stability, with weight loss of 5% at temperatures superior to 200°C (Fig S4-1 and Table S4-1 in the ESI). Then, the thermal behavior of the Janus dendrimers was studied by polarized optical microscopy (POM), equipped with heating stage, and differential scanning calorimetry (DSC), and the structure of the mesophases was studied by X-ray diffraction. The thermal and structural data are gathered in Table 1. Since several reports in bibliography show the ability of dendritic wedges to form liquid crystal mesophases,[33-34] also the thermal behavior of the starting lipophilic and hydrophilic dendron was studied; none of them shows liquid crystalline behavior (see Table S4-2 in the ESI).

POM observation of the final Janus dendrimers indicated mesomorphic behavior for **$G_1(C17)_2$-$G_3(OH)_8$**, **$G_2(C17)_4$-$G_2(OH)_4$**, **$G_2(C17)_4$-$G_3(OH)_8$** (Fig. 2). The observed focal-conic textures were all consistent with smectic A phases. Furthermore, the appearance of black zones, help to this assignation since they are related to homeotropic alignment, usual in SmA mesophases.

Table 1. Thermal and mesomorphic properties and layer spacing in the SmA mesophase.

Dendrimer	**Thermal transitions** (°C) [kJ/mol]	**d**(Å)
$G_1(C17)_2$-$G_1(OH)_2$	C 40.6 [70.5] I	
$G_1(C17)_2$-$G_2(OH)_4$	C_1 43.3 [57.9] C_2 60.3 [5.1] I	
$G_1(C17)_2$-$G_3(OH)_8$	C 43.6 [51.1] SmA 170[b] I	56
$G_2(C17)_4$-$G_2(OH)_4$	C_1 27.4[a] [11.3] C_2 42.0 [11.4] SmA 55.4 [0.6] I	50
$G_2(C17)_4$-$G_3(OH)_8$	C_1 25.7[a] [15.5] C_2 43.7 [93.1] SmA 132.7 [0.6] I	56
$G_3(C17)_8$-$G_3(OH)_8$	C_1 28.3[a] [23.9] C_2 42.7 [153.8] C_3 77.4[a] [16.4] I	

The temperatures were taken at the onset of the peak and correspond to the second heating cycle, which was recorded at 10°C/min. C: crystalline solid; SmA: smectic A mesophase; I: isotropic liquid. [a] This temperature corresponds to the maximum of the peak; [b] This data was obtained by optical observation since the transition was not detected by DSC.

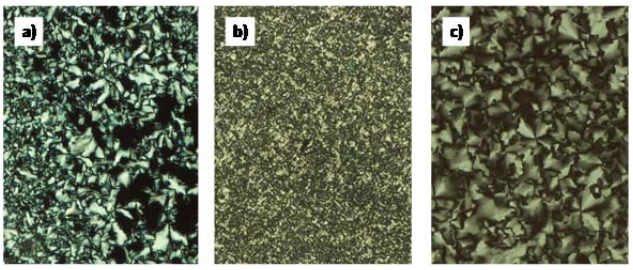

Fig. 2 Microphotographs taken at 50 ºC on cooling from the isotropic liquid for the LC Janus dendrimers. a) **$G_1(C17)_2$-$G_3(OH)_8$**, b) **$G_2(C17)_4$-$G_2(OH)_4$** (after mechanical shearing), c) **$G_2(C17)_4$-$G_3(OH)_8$**

DSC analysis yielded thermograms that confirmed the mesomorphic behavior of the three Janus compounds, **$G_1(C17)_2$-$G_3(OH)_8$**, **$G_2(C17)_4$-$G_2(OH)_4$**, **$G_2(C17)_4$-$G_3(OH)_8$**, as detected by POM observations (Fig. S4-2, S4-3 in the ESI).

All the DSC curves, during the heating process, presented a first intense endothermic peak corresponding to the transition between the crystalline phase and the isotropic liquid (compounds **$G_1(C17)_2$-$G_1(OH)_2$**, **$G_1(C17)_2$-$G_2(OH)_4$**, **$G_3(C17)_8$-$G_3(OH)_8$**) or the mesophase (compounds **$G_1(C17)_2$-$G_3(OH)_8$**, **$G_2(C17)_4$-$G_2(OH)_4$**, **$G_2(C17)_4$-$G_3(OH)_8$**). **$G_2(C17)_4$-$G_2(OH)_4$**, and **$G_2(C17)_4$-$G_3(OH)_8$** presented several endothermic peaks before the formation of the mesophase that corresponded to transitions between different crystalline forms. Moreover, they showed small peaks with low enthalpy values (0.6 kJ/mol) that correspond to the transition between the SmA phase and the isotropic liquid. This peak was not observed for the mesogenic compound **$G_1(C17)_8$-$G_3(OH)_8$**, the clearing temperature of which was deduced from POM observations.

All the three mesomorphic compounds show similar Cr-SmA transition temperatures (between 42 and 44 ºC), whereas their clearing temperatures are very different depending on the generation of the hydrophilic dendron. The highest the hydrophilic content (**$G_1(C17)_2$-$G_3(OH)_8$**), the highest the clearing temperature and, hence, the widest SmA temperature interval.

The three mesomorphic compounds were studied by X-ray diffraction in the mesophase. The diffraction patterns presented one or two maxima in the small angle region (Fig. S4-4 in the ESI). The relation between the distances of both maxima was 1:2 confirming that the mesophase was lamellar. The lamellar spacings calculated from these maxima are gathered in Table 1. These lamellar spacings were compared with calculated molecular lengths (Chem3D Ultra 7.0 included in the ChemOffice 2002 software pack), and good accordance was found, being the later slightly smaller taking into account the disordered conformations of long alkyl chains of the hydrophobic dendrons in the mesomorphic state (Table S4-3 in the ESI).

According to these data and provided the amphiphilic nature of the Janus mesogens, which promotes microsegregation to favor interactions between molecular parts of equal nature, a model is proposed in which layers are formed by the antiparallel assembly of the molecules (Fig. 3).

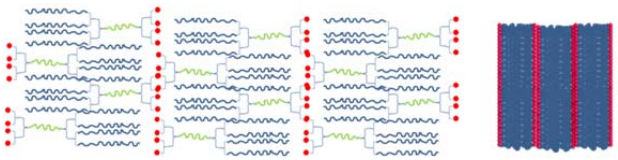

Fig. 3 Cartoon representation of the ideal arrangement of the molecules due to microsegregation.

In this arrangement, layers exhibit hydrophilic surfaces that allow interactions with contiguous layers, likely reinforced by H-bonding interactions between –OH groups. This is supported by the stabilization of the mesomorphic state for compounds containing the hydrophilic **$G_3(OH)_8$** dendron, which shows higher clearing temperatures while having similar melting temperatures than compound **$G_2(C17)_4$-$G_2(OH)_4$** (ESI, S4). Indeed, eight superficial –OH groups per dendrimer should reinforce H-bonding interlayer interactions in a greater extent than four superficial –OH groups per dendrimer, and this accounts for the broad mesomorphic range of **$G_3(OH)_8$**-containing compounds.

Self-assembly in water

The preparation of aggregates in water was undertaken for all the compounds excluding **$G_1(C17)_2$-$G_1(OH)_2$**, for which it was not possible to get aggregations at the concentration equal to its solubility limit (ESI, S5). For this purpose, the oil-in-water method was performed, which employs two immiscible phases: water and dichloromethane as the organic solvent.[32]

The morphology of the aggregates formed upon self-assembly was studied by TEM. Fig. 4 represents TEM images corresponding to all the Janus dendrimers studied, showing their corresponding morphology, which is related with a model of aggregation and the size balance between the hydrophilic and lipophilic parts of the amphiphilic molecules.

For compounds **$G_1(C17)_2$-$G_2(OH)_4$**, **$G_2(C17)_4$-$G_3(OH)_8$** and **$G_1(C17)_2$-$G_3(OH)_8$**, since the generation of the lipophilic dendron is smaller than the generation of the hydrophilic dendron, it is reasonable to apply a cone-like model. The formation of elongated micelles is observed for all three compounds, which is consistent with the theoretical model proposed for molecules with packing parameter between 1/3 and 1/2, which arrange in cylindrical and tubular micelles.[35] The morphology of the aggregates appears very similar for **$G_1(C17)_2$-$G_2(OH)_4$** and **$G_2(C17)_4$-$G_3(OH)_8$**, although the thicknesses of their corresponding bilayer models are different, being the ones formed by compound **$G_2(C17)_4$-$G_3(OH)_8$** thicker compared the ones formed by compound **$G_1(C17)_2$-$G_2(OH)_4$**. Regardless the size of the hydrophilic dendron, the Janus dendrimers containing **$G_1(C17)_2$** dendron show similar micelle dimensions.

For compounds with the same generation of both dendrons, **$G_2(C17)_8$-$G_2(OH)_8$** and **$G_3(C17)_8$-$G_3(OH)_8$**, a cylindrical model in which the lipophilic part occupies a cylinder whose base is similar to the surface of the hydrophilic part, can explain the morphology observed in TEM images. Such cylindrical geometry may favor the formation of flexible bilayers in accordance with the theoretical model proposed for molecules with packing parameter between 1/2 and 1, which should arrange into flexible bilayer or vesicles.[35] For compound **$G_3(C17)_8$-$G_3(OH)_8$** (Fig. 4), bilayers with thicknesses ranging from 9 nm to 12 nm are visible. These distances are in agreement with a distance of 6 nm estimated (Chem3D Ultra 7.0 included in the ChemOffice 2002 software pack) for the molecular length of the dendrimer. As shown in the cartoon representation in Fig. 4, the inner part of the bilayer is formed by the interaction between the aliphatic chains (light grey areas in TEM image), while the surface of the aggregates is composed by the hydroxyl groups of the hydrophilic block (dark grey areas in TEM image), in contact with the polar environment. The different thickness can be attributed to a different overlapping of the aliphatic chains. Compound **$G_2(C17)_4$-$G_2(OH)_4$** displays a very different morphology with respect to the other compounds. Aggregates, homogeneous in dimensions and with diameters around 50 nm are observed in TEM images. These structures cannot be easily explained as formed by individual bilayers. Nevertheless, considering the structural similarity of compound **$G_2(C17)_4$-$G_2(OH)_4$** with the rest of the Janus dendrimers it can be proposed that bilayer structures are indeed present but they can bend and roll-up

forming nanospheres.[36] It is significant that these nanospheres are very regular in dimensions. However, the definite nature of these aggregates is not fully clear as it is difficult to establish if the roll-up of the bilayer formed an empty vesicle or a solid packed structure.

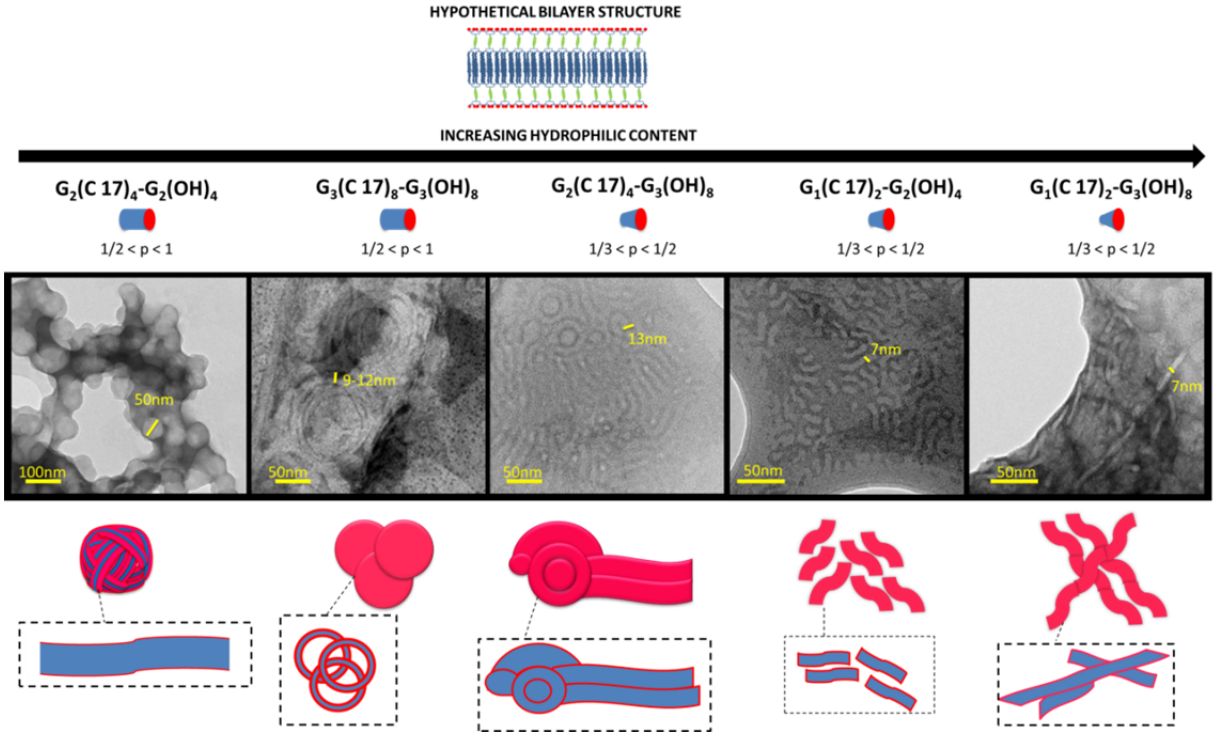

Fig. 4 TEM images corresponding to all the Janus dendrimers studied. A molecular model is assigned to each compound that represents the size balance between the hydrophilic (red) and lipophilic (blue) parts. The observed morphology is represented by an aggregation model in each case.

According to the formation of aggregates of different morphologies in water, we considered of interest to undertake preliminary studies on the possibilities of these amphiphilic Janus dendrimers to encapsulate hydrophobic molecules, which could set the basis for future studies of these systems as potential drug carriers. The encapsulation ability of the amphiphiles was tested employing Plitidepsin, a lipophilic anticancer drug supplied by PharmaMar. For this purpose, the maximum possible concentration of dendrimer and drug in water was calculated as explained in the supporting information (S6). The results of the evaluation of the concentration in solution of both the amphiphilic Janus dendrimers and Plitidepsin are collected in table 2.

Table 2 Concentration data corresponding to the encapsulation of Plitidepsin.

	Dendrimer mg/mL	Plitidepsin mg/mL	P/D mol
$G_1(C17)_2$-$G_2(OH)_4$	0.03	0.007	0.20
$G_1(C17)_2$-$G_3(OH)_8$	0.17	0.002	0.02
$G_2(C17)_4$-$G_2(OH)_4$	0.05	0.030	1.05
$G_2(C17)_4$-$G_3(OH)_8$	0.07	0.010	0.30
$G_3(C17)_8$-$G_3(OH)_8$	0.16	0.014	0.31

The lipophilic content plays a key role in the encapsulation of Plitidepsin. Analyzing the reported data, it is evident that the compounds that present the highest lipophilic content show better encapsulating ability compared to the ones composed by a bigger hydrophilic fraction. Indeed, **$G_2(C17)_4$-$G_2(OH)_4$** (column P/D in table 2) is able to encapsulate more than one mole of drug per mole of dendrimer. This positive result is probably due to the fact that this compound presents the best ratio between the lipophilic and the hydrophilic blocks; being the lipophilic part big enough to create an adequate hydrophobic environment for the drug, and the hydrophilic block sufficient to guarantee the solubilization of the whole system. Besides **$G_2(C17)_4$-$G_2(OH)_4$**, the following two compounds that show good ability to encapsulate Plitidepsin are **$G_2(C17)_4$-$G_3(OH)_8$** and **$G_3(C17)_8$-$G_3(OH)_8$**, confirming the predominant role played by the lipophilic block. Another confirmation of this hypothesis is the poor loading capacity showed by the two compounds composed by the first generation lipophilic dendron (**$G_1(C17)_2$-$G_2(OH)_4$**, **$G_1(C17)_2$-$G_3(OH)_8$**). Compound **$G_1(C17)_2$-$G_3(OH)_8$**, being the compound with the lowest lipophilic content, shows the worst encapsulating ability solubilizing only 0.02 mole of Plitidepsin per mole of dendrimer (50 molecules of dendrimers solubilize 1 molecule of drug). Probably, the small lipophilic part of this compound is not sufficient to guarantee the formation of an adequate hydrophobic environment for the encapsulation of Plitidepsin.

Conclusions

Six Janus amphiphilic compounds have been studied. All the Janus dendrimers present good thermal stability and three of them (**$G_1(C17)_2$-$G_3(OH)_8$**, **$G_2(C17)_4$-$G_2(OH)_4$**, **$G_2(C17)_4$-**

$G_3(OH)_8$) show liquid crystal behavior originating smectic A mesophases. Due to their amphiphilic nature, all the compounds, excluding $G_1(C17)_2$-$G_1(OH)_2$, self-assemble in water forming supramolecular micellar architectures or, in the specific case of compound $G_2(C17)_4$-$G_2(OH)_4$, spherical aggregates. The aggregates have been proven successful to act as host systems to encapsulate a hydrophobic drug, being the most successful amphiphilic compound $G_2(C17)_4$-$G_2(OH)_4$ that presents the higher lipophilic content but, meanwhile, a sufficient hydrophilic fraction that stabilizes the whole system in water.

Acknowledgements

This work was supported by the seventh FPTHE PEOPLE PROGRAMME,The Marie Curie Actions; ITN, no. 215884-2, the MINECO, Spain, (under Projects: CTQ2012-35692 and MAT2012-38538-CO3-01), which included FEDER funding, and the Aragón Government-FSE (Project E04). Thanks are given to: LMA Service of the Instituto de Nanociencia Aragón, University of Zaragoza (Spain) and Nuclear Magnetic Resonance, Mass Spectrometry, X-Ray Diffraction Services and Thermal Analysis Services from the CEQMA, CSIC-Universidad de Zaragoza- (Spain). E.F. acknowledges financial support from EU as an ESR fellowship in Pharmamar and A.L. thanks the MINECO for a FPU grant.

Notes and references

1 D.A. Tomalia, *Soft Matter*, 2010, **6**, 456-474.
2 W. Bosman, H. M. Janssen and E. W. Meijer. *Chem. Rev.*, 1999, **99**, 1665−168.
3 S.M. Grayson and J.M.J. Frechet, *Chem. Rev.*, 2001, **101**, 3819-3867.
4 D.A. Tomalia, H. Baker, J. Dewald, M. Hall, G. Kallos, S. Martin, J. Roecl, J. Ryder and P. Smith, *Polymer J.*, 1985, **17**, 117-132.
5 G.R. Newkome, Z. Yao, G.R. Baker and V.K. Gupte, *J. Org. Chem.*, 1985, **50**, 2003-2004.
6 C.J Hawker,.J.M.J Frechet, *J. Am. Chem. Soc.*, 1990, **112**, 7638-7647.
7 A Carlmark, C. Hawker, A. Hult, M. Malkoch, *Chem. Soc. Rev.*, 2009, **38**, 352-362.
8 F. Morgenroth, *Chem. Commun.*, 1998, 1139-1140.
9 G. Franc, A.K. Kakkar, *Chem. Soc. Rev.*, 2010, **39**, 1536-1544.
10 K. Kempe, A. Krieg, C.R. Becer, U.S. Schubert, *Chem. Soc. Rev.*, 2012, **41**, 176-191
11 C.M. Nimmo, M.S. Shoichet, *Bioconjugate Chem.* 2011, **22**, 2199-2209.
12 R.K. Iha, K.L. Wooley, A.M. Nyström, D.J. Burke, M.J. Kade, C.J. Hawker, *Chem. Rev.*, 2009, **109**, 5620–5686.
13 G.Franc A.K. Kakkar, *Chem. Eur. J.*, 2009, **15**, 5630–5639.
14 P. Wu, A.K. Feldman, A.K. Nugent, C.J. Hawker, A. Scheel, B. Voit, J. Pyun, J.M.J. Fréchet, K.B. Sharpless, V.V. Fokin, *Angew. Chem. Int. Ed. Engl.*, 2004, **43**, 3928-3932.
15 A-M Caminade, R. Laurent, B. Delavaux-Nicot, J-P Majoral, *New J. Chem.*, 2012, **36**, 217-226.
16 a) V. Percec, D.A. Wilson, P. Leowanawat, C.J. Wilson, A.D. Hughes, M.S. Kaucher, D.A. Hammer, D.H. Levine, A.J. Kim, F.S. Bates, K.P. Davis, T.P. Lodge, M.L. Klein, R.H. DeVane, E. Aqad, B.M. Rosen, A.O. Argintaru, M.J. Sienkowska, K. Rissanen, S. Nummelin, J. Ropponen, *Science*, 2010, **328**, 1009-1014. b) V. Percec, P. Leowanawat, H.-J. Sun, O. Kulikov, C. D. Nusbaum, T. M. Tran, A. Bertin, D. A. Wilson, M. Peterca, S. Zhang, N. P. Kamat, K. Vargo, D. Moock, E. D. Johnston, D. A. Hammer, D. J. Pochan, Y. Chen, Y. M. Chabre, T. C. Shiao, M. Bergeron-Brlek, S. André, R. Roy, H.-J. Gabius and P. A. Heiney, *J. Am. Chem. Soc.*, 2013, **135**, 9055-9077. c) S. Zhang, R.-O. Moussodia, H.-J. Sun, P. Leowanawat, A. Muncan, C. D. Nusbaum, K. M. Chelling, P. A. Heiney, M. L. Klein, S. André, R. Roy, H.-J. Gabius and V. Percec, *Angew. Chem. Int. Ed.*, 2014, **53**, 10899-10903. d) S. Zhang, H.-J. Sun, A. D. Hughes, R.-O. Moussodia, A. Bertin, Y. Chen, D. J. Pochan, P. A. Heiney, M. L. Klein and V. Percec, *Proc. Natl. Acad. Sci.*, 2014, **111**, 9058-9063. e) S. Zhang, H.-J. Sun, A. D. Hughes, B. Draghici, J. Lejnieks, P. Leowanawat, A. Bertin, L. Otero De Leon, O. V. Kulikov, Y. Chen, D. J. Pochan, P. A. Heiney and V. Percec, *ACS Nano* 2014, **8**, 1554-1565
17 M. Yang, Z. Zhang, F. Yuan, W. Wang, S. Hess, K. Lienkamp, I. Lieberwirth, G. Wegner, *Chem. Eur. J.*, 2008, **14**, 3330-3337.
18 J. Ropponen, S. Nummelin and K. Rissanen, *Org. Lett.*, 2004, **6**, 2495-2497.
19 a) T. Tuuttila, M. Lahtinen, N. Kuuloja, J. Huuskonen and K. Rissanen, *Thermochimica Acta*, 2010, **497**, 101-108. T. Tuuttila, b) M. Lahtinen, J. Huuskonen and K. Rissanen, *Thermochimica Acta*, 2010, **497**, 109-116.
20 I. Bury, B. Donnio, J.-L. Galliani, D. Guillon, *Langmuir*, 2007, **23**, 619-625.
21 Y. Wang, H. Xu, X. Zhang, *Adv. Mat.*, 2009, **21**,. 2849-2864.
22 I. Bury, B. Heinrich, C. Bourgogne, D. Guillon, B. Donnio, *Chem. Eur. J.*, 2006, **12**, 8396-8413.
23 a) V. Percec, M. R. Imam, T. K. Bera, V. S. K. Balagurusamy, M. Peterca and P. A. Heiney, *Angew. Chem. Int. Ed.* 2005, **44**, 4739-4745. b) M. Peterca, V. Percec, P. Leowanawat and A. Bertin, *J. Am. Chem. Soc.*, 2011, **133**, 20507-20520. c) V. Percec, M. R. Imam, M. Peterca and P. Leowanawat, *J. Am. Chem. Soc.*, 2012, **134**, 4408-4420.
24 a) U. Boas, P. M.Heegaard, *Chem. Soc. Rev.*, 2004, **33**, 43-63. b) A. K. Patri, J. F. Kukowska-Latallo, JR Baker. *Adv. Drug Delivery Rev.* 2005, **57**, 2203-2214. c) C. M. Paleos, D. Tsiourvas, Z. Sideratou, *Mol. Pharm.* 2007, **4**, 169-188. d) R. K. Tekade, P. V. Kumar, N. K. Jain, *Chem. Rev.*, 2009, **109**, 49-87. e) S. H. Medina, M. E. H. El-Sayed. *Chem. Rev.* 2009, **109**, 3141-3157.
25 Y. Wang, S.M. Grayson, *Adv. Drug Delivery Rev.* 2012, **64**, 852-865.
26 H. Hillaireau, P. Couvreur, *Cell. Mol. Life Sci*. 2009, **66**, 2873-2896.
27 O.L. Padilla de Jesus, H.R. Ihre, L. Gagne, J.M.J. Fréchet, F.C. Szoka. Bioconj. Chem 2002, **13**, 453-461.
28 A. Carlmark, E. Malstrom, M. Malkoch. Chem. Soc. Rev. 2013. 42, 5858-5879
29 H. C. Kolb, M. G. Finn and K. B. Sharpless, *Angew. Chem. Int. Ed.*, 2001, **40**, 2004.
30 H. Ihre, A. Hult, J.M.J. Fréchet, I. Gitsov, *Macromolecules*, 1998, **31**, 4061-4068.
31 Neises, B., W. Steglich, *Org. Synth.*, 1990, **Coll. Vol. 7**, 93-94.
32 V.P. Sant, D. Smith, J.-C. Leroux, *J. Controlled Release*, 1994, **97**, 301–312.
33 K.T. Al-Jamal, C. Ramaswamy, A.T. Florence, *Adv. Drug Del. Rev.*, 2005, **57**, 2238–2270.
34 B.M. Rosen, C.J. Wilson, D.A. Wilson, M. Peterca, M. R. Imam, V. Percec, *Chem. Rev.*, 2009, **109**, 6275–6540
35 T. Shimizu, M. Masuda, H. Minamikawa, *Chem. Rev.*, 2005, **105**, 1401-1444.
36 S. Hernández-Ainsa, J. Barberá, M. Marcos, J.L. Serrano, *Soft Matter*, 2011, **7**, 2560-2568.

[a] *Departamento de Química Orgánica,—Instituto de Nanociencia de Aragón (INA), Edificio I+D, Universidad de Zaragoza, 50018 Zaragoza, Spain*
[b] *PharmaMar., Madrid. 28770, Spain*
[c] *Departamento de Química Orgánica,—Instituto de Ciencia de Materiales de Aragón (ICMA) - Facultad de Ciencias, CSIC - Universidad de Zaragoza, 50009 Zaragoza, Spain. Tel: 34 976 762276; E-mail: tsierra@unizar,es*

† Electronic Supplementary Information (ESI) available: *Synthetic procedures and characterisation data, DSC thermograms, x-ray difractograms, aggregation and encapsulation procedures*. See DOI: 10.1039/b000000x/